

On the Steganographic Capacity of Selected Learning Models

Rishit Agrawal* Kelvin Jou* Tanush Obili* Daksh Parikh*
Samarth Prajapati* Yash Seth* Charan Sridhar* Nathan Zhang*
Mark Stamp*[†]

August 31, 2023

Abstract

Machine learning and deep learning models are potential vectors for various attack scenarios. For example, previous research has shown that malware can be hidden in deep learning models. Hiding information in a learning model can be viewed as a form of steganography. In this research, we consider the general question of the steganographic capacity of learning models. Specifically, for a wide range of models, we determine the number of low-order bits of the trained parameters that can be overwritten, without adversely affecting model performance. For each model considered, we graph the accuracy as a function of the number of low-order bits that have been overwritten, and for selected models, we also analyze the steganographic capacity of individual layers. The models that we test include the classic machine learning techniques of Linear Regression (LR) and Support Vector Machine (SVM); the popular general deep learning models of Multilayer Perceptron (MLP) and Convolutional Neural Network (CNN); the highly-successful Recurrent Neural Network (RNN) architecture of Long Short-Term Memory (LSTM); the pre-trained transfer learning-based models VGG16, DenseNet121, InceptionV3, and Xception; and, finally, an Auxiliary Classifier Generative Adversarial Network (ACGAN). In all cases, we find that a majority of the bits of each trained parameter can be overwritten before the accuracy degrades. Of the models tested, the steganographic capacity ranges from 7.04 KB for our LR experiments, to 44.74 MB for InceptionV3. We discuss the implications of our results and consider possible avenues for further research.

*Department of Computer Science, San Jose State University

[†]mark.stamp@sjsu.edu

1 Introduction

The field of information hiding includes watermarking and steganography, which use similar techniques, but for different purposes [28]. In digital watermarking, we want to hide information in a digital object, typically for the purpose of identifying the object. For example, we might add a unique digital watermark to each copy of a confidential pdf files that we distribute. Then, if a copy of the pdf is leaked to an unauthorized party, we could read the watermark to determine the source of the leak.

In contrast to watermarking, steganography consists of hiding information for the purpose of communication. For example, if we want to communicate with someone in a repressive country, we could hide information in a digital image of, say, a cat. If the recipient knows where and how to read the hidden information, we can communicate on topics that would otherwise be censored.

Machine learning (ML), which can be considered as a subfield of Artificial Intelligence (AI), enables computers to learn important information from training data [29]. Today, ML models are widely used to deal with a vast array of problems, including speech recognition, image recognition, sentiment analysis, language translation, and malware detection, with new applications being constantly developed. Deep learning (DL) models are the subset of ML models that are based on neural networking techniques—they are “deep” in the sense of having multiple layers.

Machine learning models are of interest in the context of steganography for the following reasons.

1. Machine learning models are rapidly becoming ubiquitous. For example, learning-based voice-activated systems were used by more than 3.25 billion people in 2021 [2].
2. The steganographic capacity of most ML models is likely to be high. Models typically include a large number of weights or other trained parameters, and learning models do not typically require high precision in their trained parameters. For example, the most popular algorithm used to train a Support Vector Machine (SVM) is Sequential Minimal Optimization (SMO), and the efficiency of this algorithm relies on the fact that limited precision suffices [29]. As another example, in neural networking-based models, many neurons tend to atrophy during training, with such weights contributing little to the trained model. By relying on such redundant neurons, the authors of [33] show that they can hide 36.9 MB of malware within a 178 MB AlexNet architecture, with only a 1% degradation in performance. These changes do not affect the structure of the model and the embedded malware was not detected by any of the anti-virus systems tested.
3. Machine learning models may be an ideal cover media for advanced malicious attacks. For example, in addition to simply embedding malware in a learning model, it is conceivable that a specific predetermined input to the model could be used to trigger the embedded malware.

As mentioned above, many learning models do not require high precision in their trained parameters. Therefore, we propose to measure the steganographic capacity of learning models by determining the number of low-order bits of each weight that can be used for information hiding, without adversely affecting the performance of a model. Specifically, we embed information in the n low-order bits of the weights of trained models, and graph the resulting model accuracy as a function of n . As our test case, we train models on a dataset that contains 10 different malware families, with a total of 15,356 samples.

The remainder of the paper is organized as follows. Section 2 gives relevant background information. Section 3 provides an overview the dataset used in our experiments, and we outline our experimental design. Our results are presented and discussed in Section 4. Finally, Section 5 gives our conclusions, and we discuss potential topics for further research.

2 Background

In this section, we discuss relevant background topics. First, we discuss steganography, then we briefly introduce the learning models that are used in this research. We conclude this section with a discussion of relevant related work.

2.1 Steganography

The word “steganography” is a combination of the Greek roots *steganós* and *graphein*, which together translate as “hidden writing” [7]. Thus, steganography consists of embedding information in a cover media [30]. In modern practice, digital steganography consists of concealing information within seemingly innocuous data, such as images, audio, video, or network communication, among other possibilities [1].

We note in passing that cryptography protects a message by transforming it into an unintelligible format. This is in contrast to steganography, where the goal is to hide the fact that the communication represented by the hidden information has even taken place. Steganography dates at least to ancient Greece and it predates cryptography as a means of secret communication [28].

A simple example of a modern steganographic application consists of hiding information in the low order RGB bits of an uncompressed image file [28]. Since the RGB color scheme uses a byte for each of the R (red), G (green), and B (blue) color components of each pixel, there are $2^{24} > 16,000,000$ colors available. However, many of these color combination are indistinguishable to humans, and hence there are redundant bits in an uncompressed image file that can be used for steganography. In particular, the low-order RGB bits of each byte can be used to hide information, without perceptibly changing the image. Provided that the intended recipient knows which images are used for hiding information, and knows how to extract the information, communication can take place between a sender and receiver, without it being apparent that the hidden information has

been communicated. The steganographic capacity of an uncompressed image file is surprisingly large—in [28, Section 5.9.3] it is shown that the a pdf file containing the entire *Alice’s Adventures in Wonderland* book can be embedded in the low order RGB bits of a single image of Alice from the *Alice* book itself.

The image-based steganographic technique in the previous paragraph is not robust, since it is easy to disrupt the communication, without affecting the non-steganographic use of such images. If a censor suspects that the low-order RGB bits of uncompressed image files are being used for steganographic purposes, he can simply randomize the low-order bits of all such images. The information would thus be lost from images that were being used for steganography, while all other images would be unaffected in any perceptible way. Research in information hiding often focuses on creating more robust steganographic techniques.

The following three issues are relevant for a steganographic technique.

- Perceptual transparency — A steganographic process should hide information in a way that is imperceptible to human senses. This ensures that it is not obvious that the cover medium is being used for secret communication.
- Robustness — As we noted in the case of image steganography discussed above, such a system may be more useful if it is robust.
- Capacity — The amount of information that can be hidden in the cover medium is the capacity. The capacity of a steganographic technique depends on the redundancy in the cover media.

In this research, we are interested in the steganographic capacity of various learning models. Specifically, we hide information in the low-order bits of the trained parameters (i.e., weights) of selected learning models. While such a simple approach to information hiding is not robust, our work does provide a basis for designing more advanced techniques, with the analogy to image-based steganography being obvious.

2.2 Learning Models

Machine learning (ML) and deep learning (DL) are tools used in the field of artificial intelligence (AI). The general topic of ML deals with training “machines” to learn from data, and is often used for classification tasks. In our usage, DL is the subset of ML that uses Artificial Neural Networks (ANN), generally with multiple hidden layers, which is the source of the word “deep” in DL. Neural networking algorithms are designed to (loosely) mimic the structure of the human brain, and such models have proven to be very effective for solving complex problems such as image and speech recognition, natural language processing, and playing complex games at superhuman levels.

ML enables computers to learn important information, and improve based on experience, which saves humans from the inherently difficult task of extracting such information from massive volumes of data [29]. A primary goal in the field of machine learning is to enable computers to learn, while requiring minimal human intervention or assistance [26].

As mentioned above, ML techniques are applied in a wide and growing range of fields. ML techniques have become staples in the areas of data security, finance, healthcare, and so on. The subfield of DL has been particularly successful at dealing with such challenging problems as speech recognition, image classification, sentiment analysis, and language translation, among many others [6].

In recent years, DL models have achieved significant successes due to their ability to automatically extract complex patterns and representations from raw data without the requirement of extensive feature engineering. Through the process of training, DL models learn to recognize patterns and relationships in data, enabling them to often perform tasks at a higher level than had previously been achievable using “classic” ML models.

ML algorithms can be subdivided into supervised and unsupervised techniques. A supervised ML technique requires labeled data to train the model. In contrast, unsupervised machine learning techniques can be applied to unlabeled data. In this paper, we only consider supervised learning techniques; specifically, we train models to classify samples from a dataset containing 10 different malware families.

Next, we introduce each of the learning techniques that are employed in the experiments in Section 4. Specifically, we discuss Logistic Regression (LR), Support Vector Machine (SVM), Multilayer Perceptron (MLP), Convolutional Neural Network (CNN), Long Short Term Memory (LSTM) models, VGG16, DenseNet121, InceptionV3, Xception, and Auxiliary Classifier Generative Adversarial Network (ACGAN).

2.2.1 Overview of Logistic Regression

Logistic Regression (LR) models are a traditional machine learning algorithm, designed to be used for classification problems with a finite number of classes [13]. LR utilizes the sigmoid function to map features to a scale of 0 to 1. While training, the model derives coefficients for each of the variables and determines a threshold for each classification. These coefficients are analogous to the weights in a deep learning model. While simple, LR models often perform reasonably well on many classification tasks.

2.2.2 Overview of Support Vector Machine

Support Vector Machines (SVM) are a class of popular supervised learning algorithms, specifically designed for classification tasks. SVMs have strong generalization capability and robustness, and they come in both linear and non-linear forms. The SVM input layer accepts the feature vectors, and the prediction is obtained via the output layer.

The main elements of an SVM are support vectors, decision boundaries (as determined by hyperplanes), and a kernel function. The kernel function can be used to map input data into a higher-dimensional “feature space”, which enables the model to deal with non-linear relationships in terms of the input data. The

main concept behind an SVM is to find the optimal hyperplane that can best separate the different classes. Support vectors are those feature vectors that maximize the margin, where margin is defined as the minimum distance from a feature vector to the decision boundary.

The process of training an SVM involves solving a quadratic programming problem, with the Sequential Minimal Optimization (SMO) algorithm currently being the best available means to do so. Of relevance to the research reported in this paper, the SMO algorithm specifically takes advantage of the fact that the weights of a trained SVM do not require great accuracy [29].

2.2.3 Overview of Multilayer Perceptron

Multilayer Perceptrons (MLP) are a popular class of feedforward neural network architectures that are widely used for supervised learning tasks, including classification and regression [32]. MLPs consist of multiple layers of interconnected nodes, where each node receives input from the previous layer and produces output that is passed to the next layer.

The input layer of an MLP receives the input data, and the output layer produces the final prediction. In between these layers, there can be one or more hidden layers that help the model to learn complex patterns in data. Each node in the hidden layers applies a nonlinear activation function to the weighted sum of its inputs, which helps to capture non-linear relationships in the data.

MLPs are trained using backpropagation, which is an optimization algorithm that adjusts the weights of the network based on the difference between the predicted output and the actual class label [29]. The weights are updated using gradient descent, which iteratively adjusts the weights to minimize the error.

One of the main advantages of MLPs is their ability to learn complex patterns in the data, making them suitable for high-dimensional and non-linear datasets. However, since they use fully-connected layers, MLPs can be computationally expensive to train and, as with most DL models, they require a large amount of labeled data to achieve high accuracy.

2.2.4 Overview of Convolutional Neural Networks

Convolutional Neural Network (CNN) is a prominent general deep learning technique. CNNs were originally designed for images, utilizing a unique architecture, consisting of convolutional layers, pooling layers, and dense layers (also known as fully-connected layers). The first convolutional layers trains filters based on input data. These filters help distinguish basic aspects of the image. Deeper convolutional layers are trained on the output of the previous layer, which enables the model to learn more abstract features—and, ultimately, to distinguish between complex images, such as those representing “cat” and “dog”. Convolution layers are often followed by a pooling layer, which decrease the dimensionality, thereby decreasing the computational requirements. The final layer of a CNN is a dense layer that is utilized to classify [3].

In spite of their origin in image classification, CNNs are applicable to other types of data. In particular, CNNs can be expected to perform well in cases where local structure is dominant.

2.2.5 Overview of LSTM

Long Short Term Memory (LSTM) is a specific type of Recurrent Neural Network (RNN). RNNs allow previous output to be used as input, based on recurrent connections, which enables such models to have a form of memory that is absent in feedforward architectures. However, in plain vanilla RNNs, this memory tends to create gradient flow problems when training via backpropagation. One advantage of LSTMs over plain vanilla RNNs is their ability to mitigate these gradient problems when training. LSTMs achieve this improvement over generic RNNs by use of a complex gating structure [29].

We note in passing that, commercially, LSTM is one of the most successful architectures yet developed. Examples of significant applications where LSTMs have played a crucial role include Google Allo [11], Google Translate [35], Apple's Siri [14], and Amazon Alexa [9].

2.2.6 Overview of VGG16

Visual Geometry Group 16 (VGG16) is a popular computer vision model [27]. VGG16 was designed as a deep convolutional neural network, pre-trained for image classification on the ImageNet dataset.

The model derives its name from its 16 layers with trainable parameters. VGG16 includes 13 convolutional layers, five max-pooling layers, and three dense layers, resulting in a total of 21 layers. Of these 21 layers, the five max-pooling layers do not contain any trainable weights.

One unique aspect of VGG16 is its architectural uniformity. It employs convolutional layers with a consistent 3×3 filter size and a stride of one, using the same padding throughout. Additionally, max-pooling layers in VGG16 use a 2×2 filter with a stride of two. This simplicity facilitates ease of implementation and efficient training.

The generalization ability of VGG16 to images beyond its training data has made it a popular and successful model. VGG16 is commonly employed in transfer learning, where the original dense layers are replaced with new task-specific dense layers. The hidden layers, consisting of the convolutional and max-pooling layers from the original model, remain unchanged and are used as a feature extractor while training the new fully connected layers on the new data.

2.2.7 Overview of DenseNet121

DenseNet121 is a convolutional neural network architecture that belongs to the DenseNet family [10]. It consists of four dense blocks and several transition layers that involve convolution and pooling. The dense layers receive direct input from

all preceding layers within the same block, allowing for feature reuse. Transition layers are inserted between dense blocks to control the spatial dimensions and channel depth of the feature maps. A dense blocks is typically followed by an average-pooling layer, which serves to reduce the dimensionality. DenseNet121 ends with a classification head, containing a fully connected layer with a `softmax` activation.

DenseNet121 was designed to address the limitations of traditional CNN architectures, such as vanishing gradients and information flow constraints. Since its introduction in 2017, the model has been successfully applied to image classification tasks and object detection. With excellent information flow and feature reuse, DenseNet121 can capture fine-grained details and small-scale patterns throughout the network, which is crucial for image analysis. In spite of having more than six million trainable parameters, DenseNet121 is more computationally efficient and requires less memory than many other comparable CNN models, including ResNet152 and VGG16 [10].

2.2.8 Overview of InceptionV3

InceptionV3 is a prominent CNN architecture that has been very successful in the domain of computer vision. This advanced architecture was developed as an enhancement to Google’s initial Inception model, providing an innovative approach to efficient computation and the discernment of complex patterns within image data [31].

A distinguishing feature of the InceptionV3 network is its proprietary “Inception Modules.” These modules incorporate convolution operations with various kernel sizes that operate simultaneously, thereby enabling the model to efficiently learn features from the input data.

In typical applications, the input to an InceptionV3 model comprises image data, and its output layer delivers predictions across a pre-defined set of classes. The intervening layers of the architecture—including numerous convolutional layers, pooling layers, Inception modules, and fully connected layers—perform sequential transformations of the input data. This sequence facilitates the extraction of patterns and relevant features from the images.

The training of the InceptionV3 model employs backpropagation and gradient descent. Due to its complex and deep structure, it also employs advanced techniques such as batch normalization (BatchNorm) and sophisticated initialization schemes. These approaches are intended to ensure efficient training and mitigate potential issues such as the vanishing gradient problem.

The InceptionV3 architecture is known for its balance of computational efficiency and high accuracy, performing effectively even with a large number of classes and when handling high-resolution image data. Nevertheless, training the InceptionV3 network can be computationally intensive, and typically requires a substantial volume of labeled data.

2.2.9 Overview of Xception

The Xception model is a deep CNN that is an expansion of the Inception architecture. The convolutional blocks that make up the Xception architecture each have multiple convolutional layers [5]. The convolutions that the Xception model employs are divided into two categories, namely, depthwise convolutions and pointwise convolutions. Pointwise convolutions utilize a 1×1 convolution to mix the outputs of depthwise convolutions, whereas depthwise convolutions apply a single filter to each channel-wise $n \times n$ spatial convolution independently. A matrix of pixel values is used to represent the input image, and each pixel contains RGB color information, which is passed through an initial convolution block. Global average pooling is employed, where the average value of each feature map is used to create a single value for each channel. The final output layer consists of a fully connected layer followed by a `softmax` activation function for classification tasks.

2.2.10 Overview of ACGAN

Auxiliary Classifier Generative Adversarial Network (ACGAN) is a specific type of Generative Adversarial Network (GAN) that is used when the data consists of multiple classes. In addition to classification, GANs can be used to generate new “deep fake” data instances that resemble the training data.

A GAN has two neural networks, a generator and a discriminator, that compete in an adversarial zero-sum game. The generator produces new pieces of data that are as close to the training data as possible. The discriminator attempts to determine whether the input it receives—some of which comes from the generator and some of which comes from the actual training data—is generated or authentic. The discriminator and generator weights are updated in a way that incentivizes the generator to produce “fake” data that is similar to the training data, and incentivizes the discriminator to accurately diagnose if a sample is fake or real [8].

An ACGAN works similarly, except that the discriminator also returns the class it thinks the data belongs to. The ACGAN incentivizes the generator to produce believable fakes that conform well to a specific class, while the discriminator is incentivized to accurately diagnose fake samples and classify the data.

2.3 Related Work

In the paper [33], a technique that the authors refer to as “EvilModel” is used to hide malware in a neural network model. In one example, a malware sample of size 36.9 MB is embedded in a specific model, and the accuracy of the model is reduced by about 1%. The authors of [33] embed malware in a learning model by carefully selecting weights that have minimal effect on model performance, and then overwrite these weights with the malware sample.

The paper [34] is a continuation of the work in [33]. Among other results, in [34], malware is embedded in the least significant bits of model weights, and an “embedding rate” of slightly more than 48% is achieved.

The paper [15] considers a technique that its authors call “StegoNet.” Among other contributions, this paper includes experiments consisting of modifying the least significant bits of model weights, and they propose a plausible trigger mechanisms for malware that is embedded in a machine learning model.

Here, we consider the problem of embedding information in the least significant bits of model weights. In comparison to [34], we are generally able to achieve relatively high embedding rates with no significant decrease in model performance. In contrast to both [34] and [15], we consider far more model types, and our analysis is much more thorough, as we provide graphs explicitly showing the tradeoff between the number of bits overwritten and model accuracy.

The work presented in this paper is a continuation of the work in [36], where the steganographic capacity of a Multilayer Perceptron (MLP), a Convolutional Neural Network (CNN), and a specific Transformer model are analyzed. Here, we consider the models introduced in Section 2.2, above, and provide a detailed analysis of the steganographic capacity of each.

3 Implementation

In this section, we introduce the malware dataset used to train our learning models. Then we provide details on our experimental design. Our experimental results are given in Section 4, below.

3.1 Dataset

Malware samples that are closely related can be grouped into families. Malware samples within a family generally have similar functionality, behavior, and code structure. Members of a given family typically share a core code base that contains common functions, routines, and behavior. Malware families tend to evolve over time, and new families can branch off from existing families.

In this research, we consider a malware dataset obtained from VirusShare [12]. This dataset contains more than 500,000 malware executables. From this dataset of 500,000 malware executables, we consider the top 10 most numerous families—these malware families and number of samples per family are listed Table 1. Note that the dataset is imbalanced, with the most numerous of the 10 families containing more than 17% of the samples, while the least numerous has slightly over 7% of the samples.

Next, we briefly describe each of these families; for more details, see [36]. These families include several different categories of malware, including viruses, worms, and Trojans.

Table 1: Malware families

Family	Samples	Fraction of total
Adload	1225	0.0798
BHO	1412	0.0920
Ceeinject	1084	0.0706
OnLineGames	1511	0.0984
Renos	1567	0.1020
Startpage	1347	0.0877
VB	1110	0.0723
VBinject	2689	0.1751
Vobfus	1108	0.0721
Winwebsec	2303	0.1500
Total	15,356	1.0000

Adload is an adware program that displays unwanted advertisements on a web browser [25].

BHO, is a type of add-on or plugin for web browsers, such as Internet Explorer. While there are many legitimate BHOs, the malware version can perform unwanted actions, such as redirecting web traffic or displaying unwanted ads [19].

Ceeinject injects itself into legitimate processes running on a Windows operating system, allowing it to execute its malicious code undetected [17].

OnLineGames is a Trojan that mimics an online game [24].

Renos is designed to trick users into purchasing fraudulent security software or services [18].

Startpage is a family of Trojans that modifies a user’s web browser settings, such as the homepage and search engine, without the user’s consent [23].

VB is a simple Trojan that spreads a worm by copying itself to removable drives, network shares, and other accessible file systems [16].

VBinject is a general technique that is applied by malware author to inject malicious program into legitimate Windows processes [20].

Vobfus is a malware family that downloads other malware, such as Zbot, onto a victim’s computer [21].

Winwebsec is designed to trick users into purchasing fraudulent security software or services. It displays false alerts and warnings about supposed security threats [22].

We consider several types of feature vectors, depending on the requirements of the particular model under consideration. For our feedforward models (LR, SVM, MLP, ACGAN), we extract a relative byte histogram from each sample. For our

image-based models (CNN, VGG16, DenseNet121, InceptionV3, Xception), we treat the raw bytes of an `exe` file as an image. For example, if a model uses 64×64 images, we place the first 4096 bytes of an `exe` into a 64×64 array (padding with 0 bytes, if necessary) which we then treat as an image. For our model that requires sequential data (LSTM), we use the first n bytes of each `exe` file. Note that in all cases, these feature vectors are trivial to generate, and require no costly disassembly or dynamic analysis.

3.2 Model Training

A similar training and testing procedure is used for each of the 10 learning models considered. First, we train each model with labeled data and test the trained model, which establishes a baseline level of performance. In this phase a grid search is performed over a set of reasonable hyperparameter values. Accuracy is used as our measure of performance.

After the initial training and testing, data is inserted into the low-order n bits of the weights, which, on average, changes about half of the bit values. For each n , the performance of the model is re-evaluated using the same data and accuracy metric as for the unmodified model. This allows for a direct comparison of the results for each n . We graph the accuracy as a function of n .

4 Steganographic Capacity Experiments

In this section, we consider the steganographic capacity of each of the 10 models discussed in Section 2.2. As mentioned above, to measure the steganographic capacity, we embed information in the low-order n bits of the model weights, and we graph the accuracy as a function of n . In all cases, the information that we hide is extracted from the pdf version of the book *Alice's Adventures in Wonderland* [4].

For each deep learning model, we consider the following cases.

1. Only the output layer weights are modified
2. The weights of all hidden layers are modified
3. All of the model weights are modified

For selected models, we also consider the effect of overwriting the weights of individual layers. In addition to graphing the model accuracy as a function of n , we provide a capacity graph, that is, the number of model bits that have been overwritten for each n .

To determine the overall capacity of a model, we find the number of bits n that must be overwritten for a 1% drop in accuracy, as compared to the original trained model, which has no bits of its weights overwritten. We then use $n - 1$ as the per-weight steganographic capacity, and the total capacity (in bits) is determined by multiplying the number of weights by $n - 1$. We give the capacity in kilobytes (KB) or megabytes (MB), as appropriate.

4.1 LR Experiments

This model utilized the `LogisticRegression()` class from the `sklearn` package in Python `scikit-learn`. The class has 4 different hyperparameters, all of which were tested via grid search and optimized. The hyperparameter values tested are given in Table 2, with the values in boldface yielding the best results.

Table 2: LR hyperparameters tested

Hyperparameter	Values tested
<code>solver</code>	lbfgs , saga, liblinear
<code>penalty</code>	elasticnet, l2
<code>C (regularization)</code>	0.2, 0.3, 0.5, 0.7, 0.8
<code>max_iter</code>	50, 80, 100 , 120, 200, 500

For this 10-class classification problem, the model achieves a respectable accuracy of 0.8717 on the validation set. From the confusion matrix for our model, which appears in Figure 13 in the appendix, we see a similar spread of errors, as compared to the other models tested, with slightly poorer performance in identifying WinWebSec viruses.

Since LR models only have one layer of coefficients, we can only overwrite the bits in that layer; the graph of these results are given in Figure 1. There is no drop in model accuracy when $n \leq 22$ bits are overwritten, with about a 2% drop at $n = 23$. Therefore, we can overwrite the 22 low-order bits of each weight with no loss in performance and hence we deem $n = 22$ as the steganographic capacity per weight of this model. Since the model has 2560 weights, the total steganographic capacity is $22 \cdot 2560 = 56,320$ bits, or 7.04 KB.

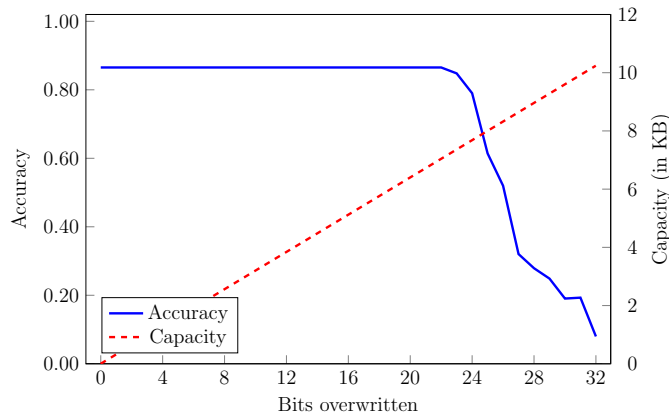


Figure 1: LR steganographic capacity graph

4.2 SVM Experiments

The `svm.SVC()` function from the `sklearn` module from `scikit-learn` was used for the training and testing of our SVM model. The hyperparameters that we tested are listed in Table 3, with the selected values in boldface. For example, the SVM model with a `C` value of 1 yielded the best results, and the `linear` kernel was selected, with a `gamma` value of 0.1.

Table 3: SVM model hyperparameters tested

Hyperparameter	Values tested
<code>C</code> (regularization)	0.1, 1 , 10
<code>kernel</code>	linear , rbf
<code>gamma</code>	0.1 , 1, 10

Based on the confusion matrix for the SVM model, which appears in Figure 14 in the appendix, the model performs similarly to the other models, with the highest level of confusion for the `VBinject` class of viruses. Also, the SVM model outputs a classifying accuracy of 0.8264 for the `Adload` class, which is lower than the most accurate of our models.

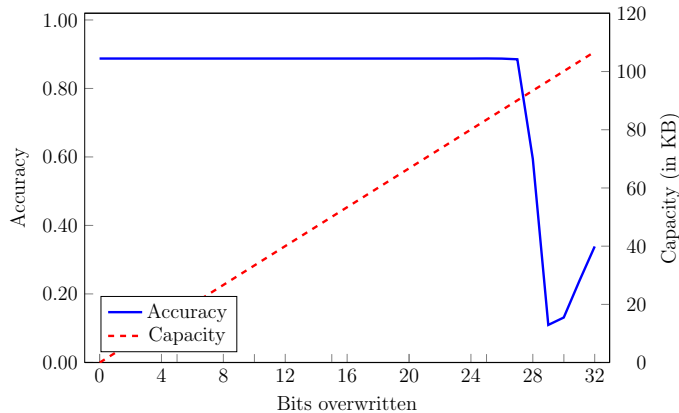


Figure 2: SVM steganographic capacity graph

The overall accuracy of our SVM model is 0.8870. An SVM consists of a single “layer” of coefficients, which correspond to the weights of a deep learning model. Furthermore, SVM coefficients are within the range of -1 to 1 , with a higher magnitude indicating a larger importance in determining the decision boundary. The model was able to withstand the overwriting of 27 bits before experiencing a significant drop in accuracy, which is a slightly higher per-weight capacity than any of the deep learning models considered. The SVM model contains 26,703 coefficients (i.e., weights) and hence we calculate the steganographic capacity of the model to be 90.12 KB.

4.3 MLP Experiments

The MLP results we present here are from [36]; we include these results for the sake of comparison. The `MLPClassifier()` from the `sklearn.neural_network` module was used to train and test our MLP model. The hyperparameters tested are listed in Table 4, with the selected values appear in boldface. Note that a model with two hidden layers, with 128 and 10 neurons, respectively, was best. Also, the `logistic` function was selected as our activation function.

Table 4: MLP model hyperparameters tested

Hyperparameter	Values tested
<code>hidden_layer_sizes</code>	(64, 10), (96, 10), (128, 10)
<code>activation</code>	identity, logistic
<code>alpha</code>	0.0001, 0.05
<code>random_state</code>	30, 40 , 50
<code>solver</code>	adam
<code>learning_rate_init</code>	0.00001
<code>max_iter</code>	10000

The results obtained when overwriting the low order bits of all weights of our trained MLP model are summarized in Figure 3(c). We observe that the original accuracy for the model is 0.8417, and the performance of the model is unchanged when the low-order 19 bits of the weights are overwritten, while there is a 1% drop in performance when 20 bits are overwritten. Overwriting more bits causes the accuracy to drop substantially.

Figures 3(a) and (b) are the results when overwriting the output and internal layer weights, respectively. The results in these two cases are similar—although not identical—to the results for all weights, discussed above.

There are 100 weights in the output layer, and 34,048 weights in the hidden layer, which makes the total number of weights 34,148 in this particular MLP model. Since we can hide information in 19 bits of the all of the weights, we find that the steganographic capacity of this MLP model is approximately 81.10 KB.

4.4 CNN Experiments

A Keras `Sequential` model with the `Conv2D()`, `Dense()`, and `MaxPooling2D()` layers provided by `tensorflow.keras.layers` was used to train our CNN model. After testing the hyperparameters listed in Table 5, we found those in boldface to be the optimal choices for our model. The 12 layers in our CNN consisted of four `Conv2D()` and `MaxPooling2D()` layers, along with two `Dense()` layers. The other two layers are dropout and flattening layers, for which the placement and dropout rate were tested. The activation function for the last dense layer is `softmax`, with the other convolution layers using `ReLU` as their activation functions.

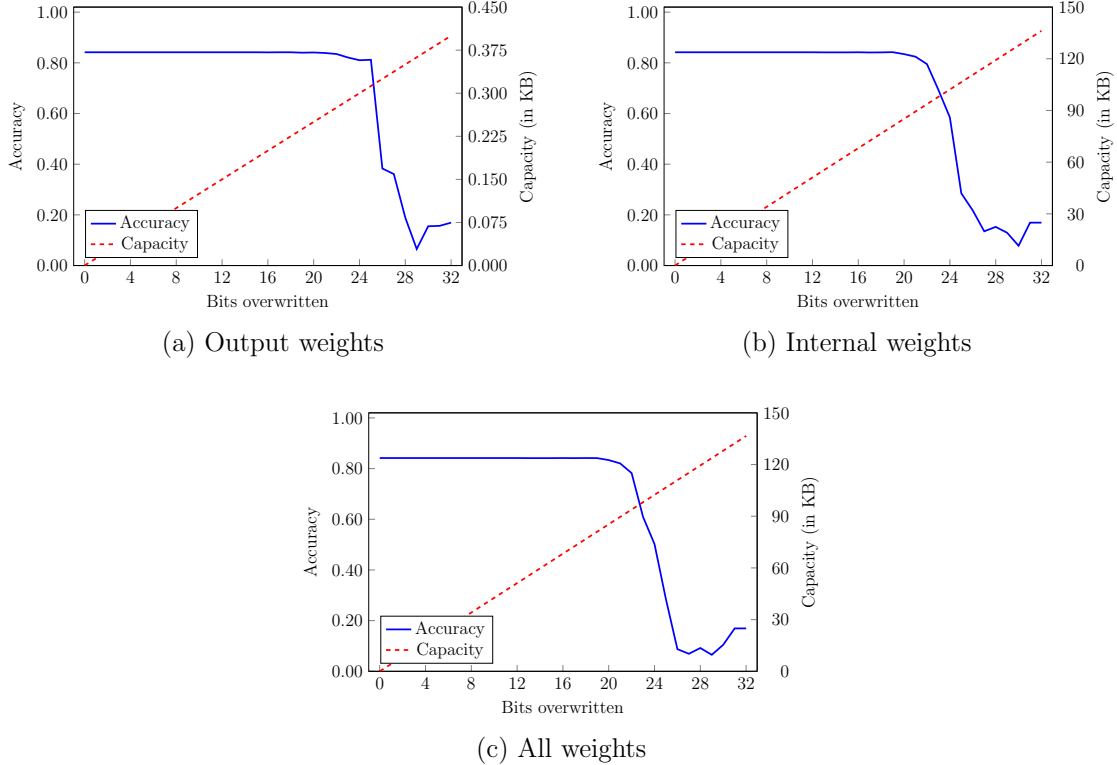


Figure 3: MLP steganographic capacity graphs [36]

Table 5: CNN hyperparameters tested

Hyperparameter	Values tested
layers	6, 8, 10 12
activation	ReLU, softmax , sigmoid
dropout rate	0.1, 0.2 , 0.3, 0.4, 0.5
learning rate	0.001 , 0.1

Our CNN model achieves an accuracy of 0.8925. From the accuracy and loss graph in Figure 4, we detect no signs that the model is overfitting the data.

The confusion matrix for our best CNN model appears in Figure 15 in the appendix. From the confusion matrix, we observe that the VB and VBInject viruses account for the majority of errors on the test set. This is reasonable, as these two families are relatively similar.

The results of overwriting the low-order bits for different layers can be seen in Figure 5. In the case of all model weights, the accuracy first drops when we overwrite 21 bits, and hence we denote the per-weight capacity as 20 bits. Our CNN model has 5130 weights in the output layer and 1,484,544 weights in the internal layers, for a total of 1,489,674 weights. This give us an overall steganographic capacity of approximately 3.72 MB

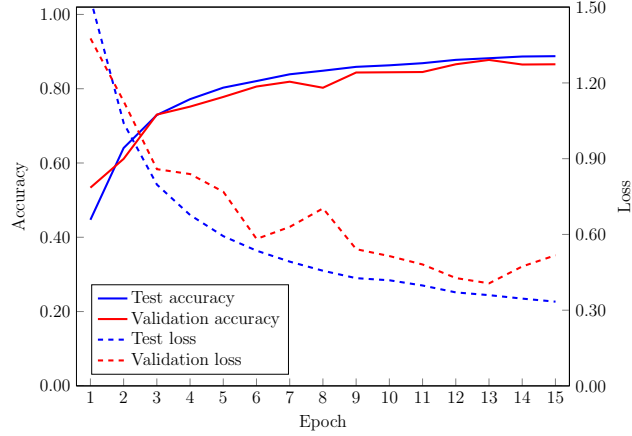


Figure 4: Test and validation graphs for CNN

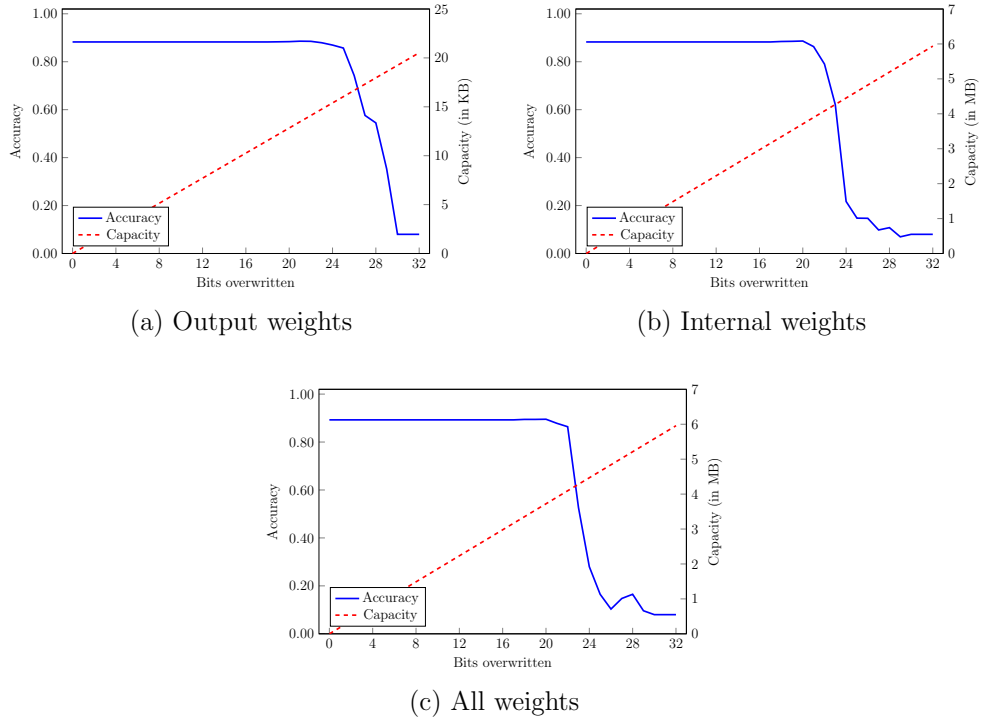


Figure 5: CNN steganographic capacity graphs

4.5 LSTM Experiments

The LSTM() function from the `keras` module was used for training and testing our LSTM model. Table 6 shows the hyperparameters tested while training, and the boldface entries indicate the combination that yielded the best results. The confusion matrix for our best LSTM model appears in Figure 16 in the appendix.

As feature vectors for our LSTM, we use the first N bytes of the `exe` files,

Table 6: LSTM model hyperparameters tested

Hyperparameter	Values tested
batch_size	16, 32 , 64, 128
activation	tanh , ReLU
epoch	5, 10 , 12
optimizer	RMSprop, adam
learning_rate	0.0001, 0.001
LSTM_units	64, 128, 512
dense_layer_units	64, 128 ,
sequence_length	150, 200, 300 , 350, 400

where each byte is converted to the range of 0 and 1 by treating the byte value as an integer and dividing by 255. We experimented with the different values of N as listed in Table 6 and found that $N = 300$ gave us the best results. Note that this model is extremely lightweight, and hence it is not surprising that it yields slightly less accurate results, as compared to other models tested.

When overwriting low-order bits of all weights, the validation accuracy is slightly more than 0.78 up to 24 bits. However, the accuracy drops about 4% when 25 bits have been modified per weight, before plummeting at 26 bits, as shown in Figure 6(c). The results for the output and internal layers are similar.

With 1,119,626 trainable parameters, the weights were split into an LSTM layer and two dense layers. The majority of the units are found in the LSTM layer (containing a total of 1,052,672) in this particular LSTM model. The first dense layer has 65,664 weights while the output dense layer only possess 1290. Based on overwriting the 24 low-order bits, the total steganographic capacity of this LSTM is about 3.36 MB.

4.6 VGG16 Experiments

The `VGG16()` model pre-trained on ImageNet from the `tf.keras.applications` module was used to train and test our VGG16 model. Since this is a transfer learning model, we replaced the old dense layers with a new dense layer that has 10 units, each unit corresponding to one of our output classes. The output layer uses a `softmax` activation function. The hyperparameters tested are listed in Table 7, with the selected values in boldface. Note that most of the hyperparameters of the model are predetermined due to transfer learning. The confusion matrix for our best VGG16 model appears in Figure 17 in the appendix.

For all of the pre-trained models considered here (i.e., VGG16, DenseNet121, InceptionV3, and Xception) we refer to the weights that are re-trained for our malware classification problem as the “trained weights.” These are in contrast to the pre-trained weights, which do not change from the pre-trained models.

Only the output layer weights of this model were retrained for our malware classification problem. From the graph in Figure 7(a), we see that our VGG16

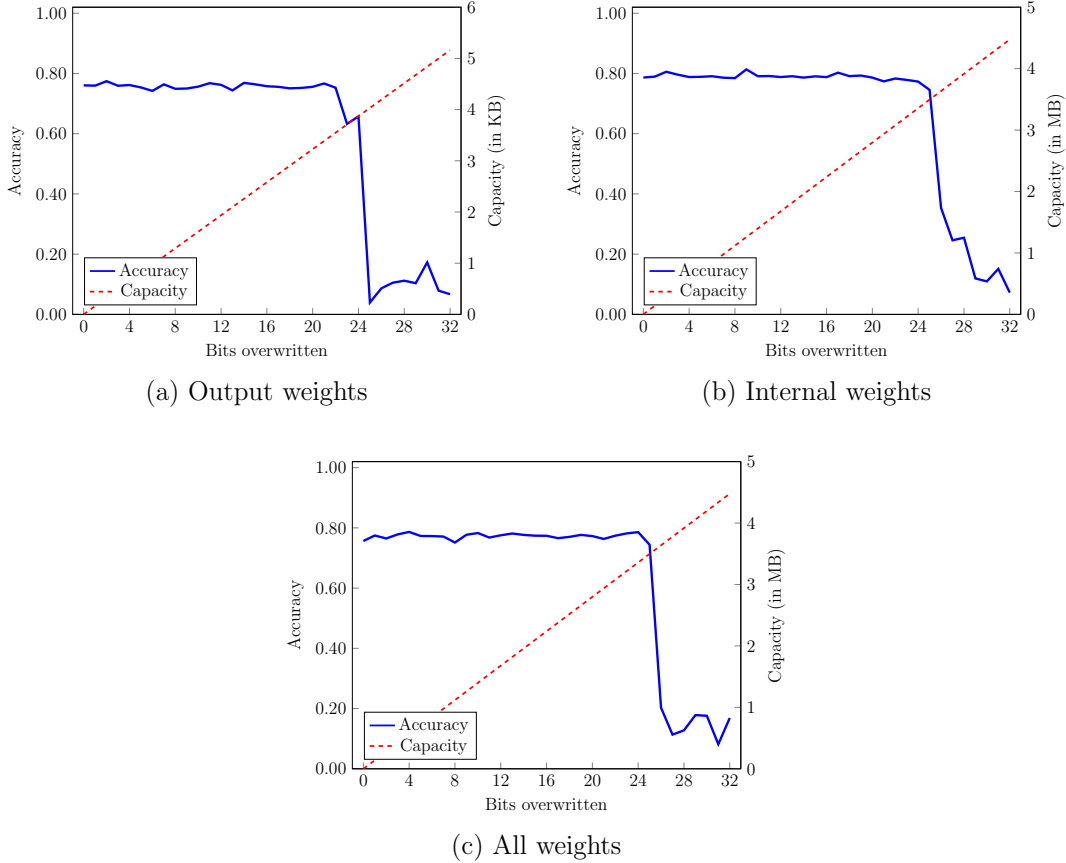


Figure 6: LSTM steganographic capacity graphs

Table 7: VGG16 model hyperparameters tested

Hyperparameter	Values tested
random_state	100, 120 , 130
solver	adam
learning_rate_init	0.001, 0.01
max_iter	50, 75, 100

model accuracy is maintained when 21 bits of the trained weights are overwritten, with a drop of more than 2% at 22 bits, and a larger drop thereafter. Thus, the per-weight capacity is 21 bits when only trained weights are considered. Since the output layer has 5130 weights, this gives us a capacity of 13.47 KB.

Figure 7(b) gives capacity results for the pre-trained weights, while Figure 7(c) contains the results for all weights. In both of these cases, the per-weight capacity is 20 bits. The hidden layer of our VGG16 implementation has 14,714,688 weights, and hence the total number of weights is 14,719,818 in our VGG16 model. considering all weights, this gives us a capacity of almost 36.8 MB.

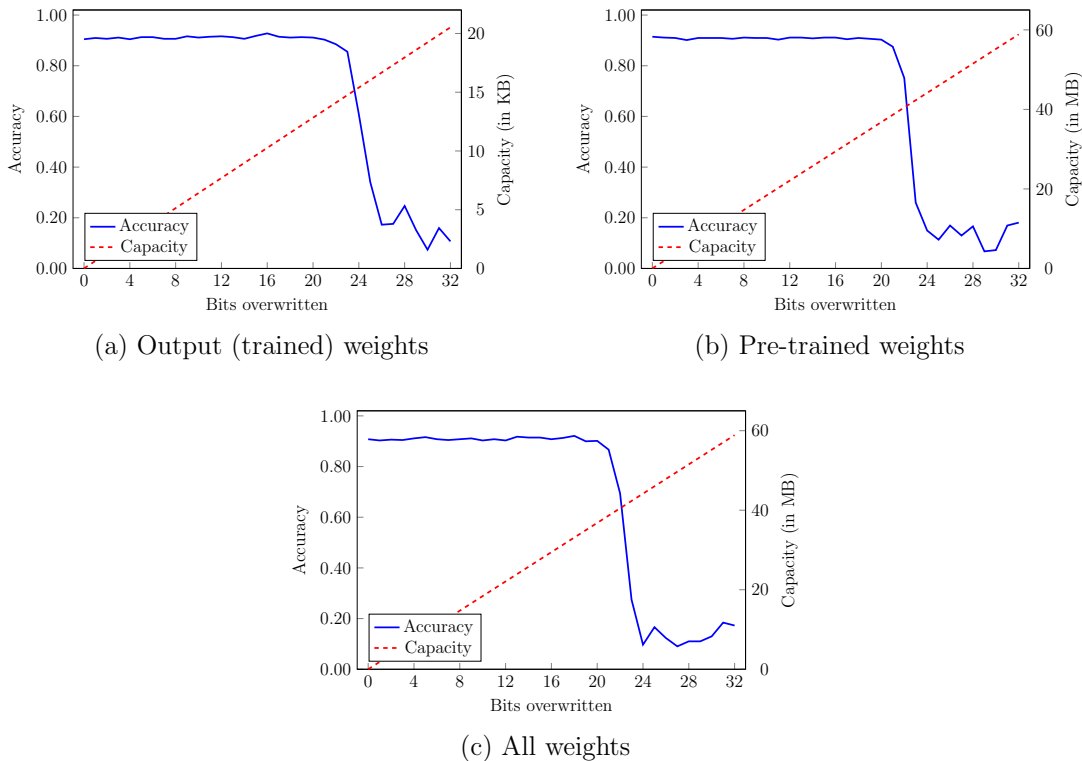


Figure 7: VGG16 steganographic capacity graphs

Figure 18 in the appendix gives the steganographic capacity results for each of the 13 individual layers in our VGG16 model. In each case, these graphs follow a similar pattern, and hence we observe no dramatic differences between the layers, with respect to our steganographic capacity experiments.

4.7 DenseNet121

`DenseNet121()` from the `tensorflow` module was used for training and testing. Table 8 shows the hyperparameters tested, and the boldface entries indicate the combination that attained the best results. The confusion matrix for our best DenseNet121 model appears in Figure 19 in the appendix.

From Figure 8(c) we observe that the model accuracy is about 0.88 and that overwriting 20 bits of the trained weights provides no loss in accuracy, but overwriting 21 bits results in a 2% drop, with further declines thereafter. Thus, the per-weight steganographic capacity of our DenseNet121 model is 20, when considering the trained weights.

DenseNet121 contains 7,571,530 total parameters, but only 700,106 weights are trainable. Thus, when modifying the trained weights, the model has a capacity of about 1.75 MB, based on a per-weight capacity of 20 bits.

Table 8: DenseNet121 hyperparameters tested

Hyperparameter	Values tested
batch_size	16, 32, 64 , 128
activation	ReLU
kernel_regularizer	12 (0.01)
epoch	5, 10 , 12
optimizer	adam
learning_rate	0.0001 , 0.001
dense_layer_units	64, 128, 512
input_shape	64, 128, 224, 64

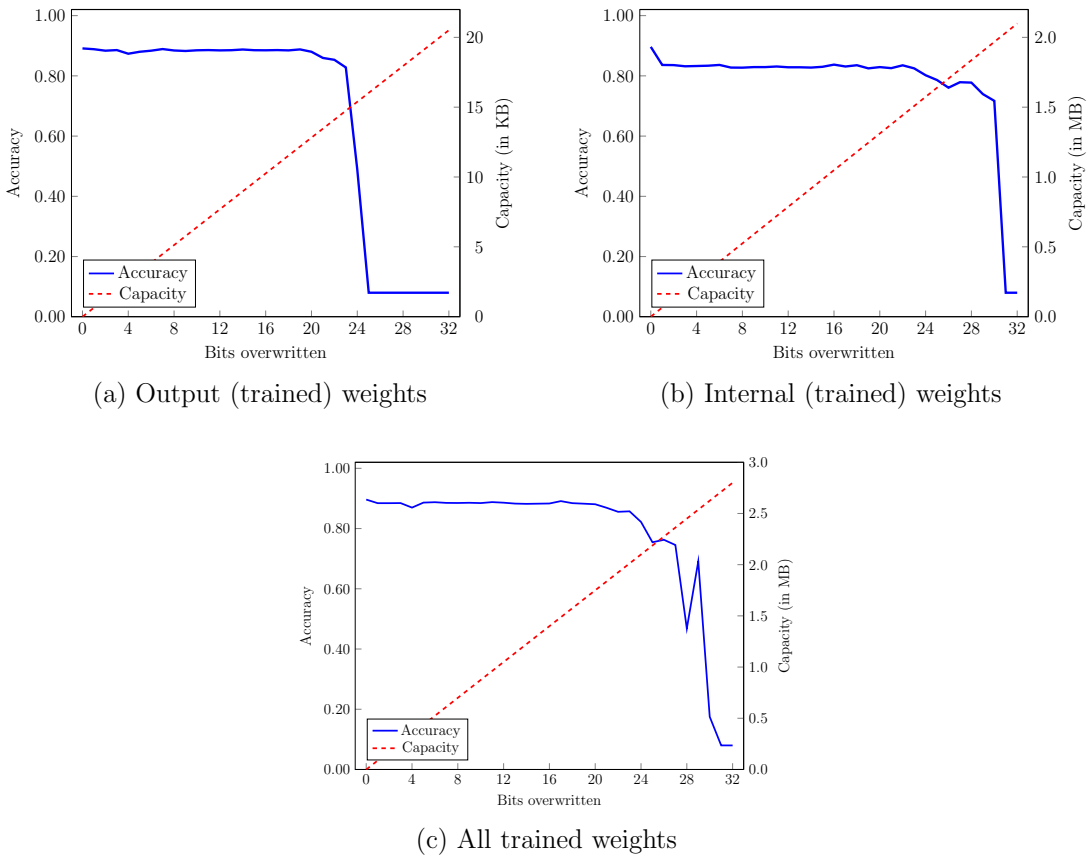


Figure 8: DenseNet121 steganographic capacity graphs

4.8 InceptionV3

The InceptionV3 pre-trained model from the `Keras` library was utilized for our training and testing. This model is based on transfer learning, with fine tuning applied to the final layers (i.e., the output and dense layers) for our specific malware classification problem. The hyperparameters tested are listed in

Table 9, with the selected values in boldface. Since InceptionV3 is a pre-trained model, only three hyperparameters tested, namely, `epochs`, `batch_size`, and `learning_rate`. The confusion matrix for our best InceptionV3 model appears in Figure 20 in the appendix.

Table 9: InceptionV3 hyperparameters tested

Hyperparameter	Values tested
<code>epochs</code>	2, 4 , 5, 8
<code>batch_size</code>	32, 64 , 128
<code>learning_rate</code>	0.001, 0.0001 , 0.0005

Figure 9(c) summarize the effect of hiding data in all trained weights of our InceptionV3 model. The model’s initial accuracy is approximately 0.9004 and remains above 0.89 until we have overwritten the 26 least-significant bits, which causes only a slight decline in accuracy to 0.88, with more substantial drops thereafter. Thus, with respect to the trained weights, we consider 25 bits as the per-weight capacity of this model.

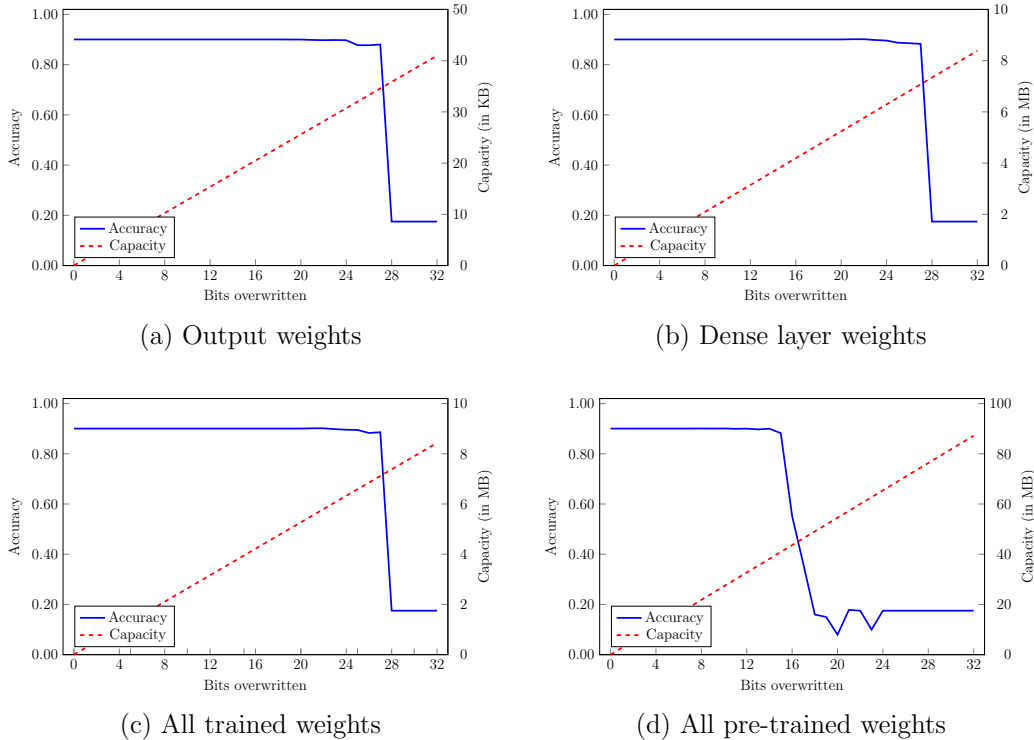


Figure 9: InceptionV3 steganographic capacity graphs

Our InceptionV3 model has 10,240 weights in the output layer, and 2,097,152 weights in the dense layer, for a total of 2,107,392 trained weights. With a

per-weight capacity of 25 bits, this gives us a total steganographic capacity of approximately 6.59 MB in the trained weights.

In Figure 9(d), we have the capacity graph for the pre-trained weights of the InceptionV3 model. Interestingly, the pre-trained weights have a much lower per-weight steganographic capacity, as compared to the trained weights. For the pre-trained weights, we observe a drop of about 1% in accuracy at 15 bits, followed by a steep drop at 16 bits, and hence we consider 14 bits as the per-weight capacity with respect to the pre-trained weights. There are 21,802,784 weights in the pre-trained InceptionV3 layer, so even with its lower per-weight capacity of 14 bits, the total steganographic capacity of the pre-trained weights is large, at 38.15 MB.

4.9 Xception

The Xception pre-trained model from the `tensorflow.keras` module was used for our Xception experiments. The hyperparameters tested are listed in Table 10, and the combination that yielded the best result appear in boldface. Note that both `softmax` and `ReLU` activation functions were utilized in the hidden layers, and the input data was reshaped to fit the input size of (256, 256, 3). The confusion matrix for our best Xception model appears in Figure 20 in the appendix.

Table 10: Xception model hyperparameters tested

Hyperparameter	Values tested
<code>input_shape</code>	(256,256,3), (299,299,3)
<code>activation</code>	ReLU, softmax
<code>num_classes</code>	10
<code>batch_size</code>	16, 32, 64
<code>epochs</code>	5, 7, 10 , 15
<code>learning_rate</code>	0.001, 0.0001
<code>kernal_regularizer</code>	l2(0.01)
<code>test_split</code>	0.2

Figure 10(c) provides a summary of our experimental results when the low-order bits of all weights are overwritten. The initial accuracy is about 0.88, and there is a marginal—but inconsistent—decline at small values of n , with the consistent decline beginning when 21 bits of the trained weights are overwritten. Thus, we take $n = 20$ as the per-weight steganographic capacity of our Xception model, with respect to trained weights.

In this particular Xception model, the hidden layers have 29,046 weights, and the output layer contains 5130 weights, for a total of 34,176 trained weights. Based on a per-weight capacity of 20 bits, we find the steganographic capacity is 85.44 KB in the trained weights.

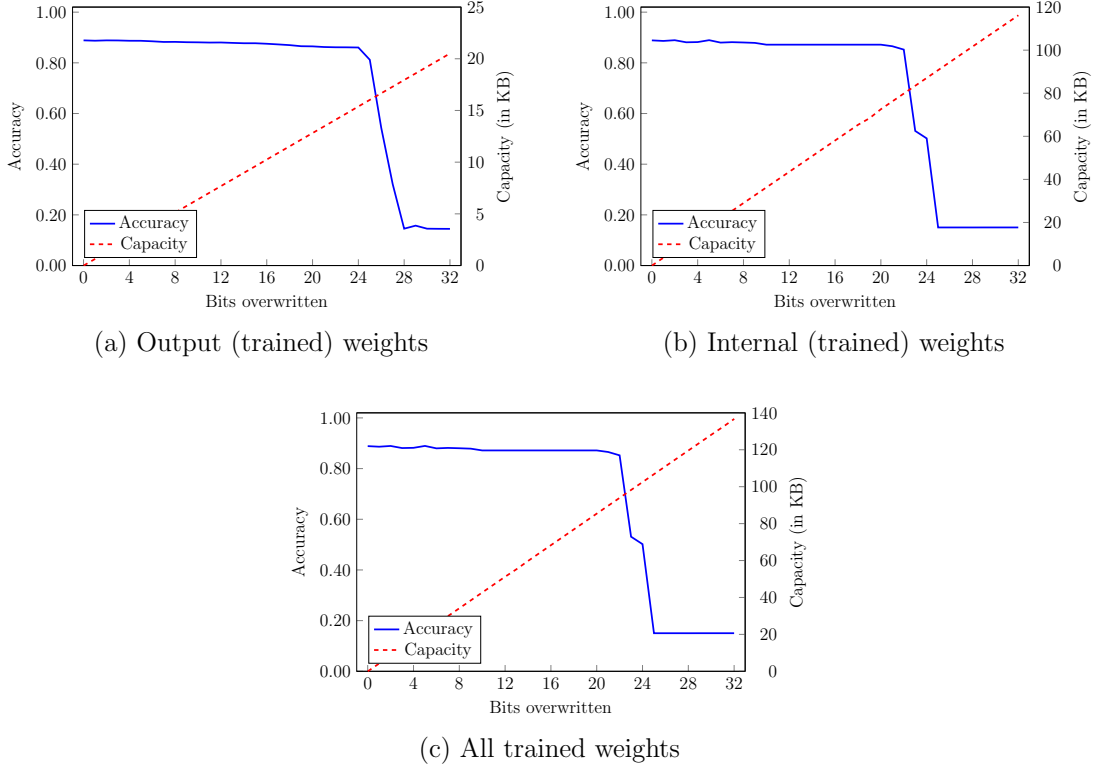


Figure 10: Xception steganographic capacity graphs

4.10 ACGAN

For our ACGAN, we use the `Sequential` model from `keras.models` to train the discriminator and generator. The discriminator of the trained ACGAN, is then used as the classifier in our steganographic capacity experiments. The hyperparameters tested for the model are listed in Table 11, with the selected values in boldface. The confusion matrix for our best ACGAN discriminator model appears in Figure 22 in the appendix. Note that the ACGAN generator plays no role in our capacity calculations, below.

Table 11: ACGAN discriminator hyperparameters tested

Hyperparameter	Values tested
<code>pad-size</code>	same
<code>batch size</code>	32 , 128, 256
<code>max-epochs</code>	10000, 14000
<code>random_state</code>	10, 50, 100
<code>momentum</code>	0.5, 0.8
<code>learning_rate_init</code>	0.0001 0.0002
<code>solver</code>	adam

The results obtained when hiding information in the low-order bits of the weights of our trained discriminator model are summarized in Figure 11. We observe that the original accuracy for the model is approximately 0.8469, and the performance of the model declines by slightly more than 1% when 21 bits are overwritten, and hence we consider $n = 20$ to be the per-bit capacity.

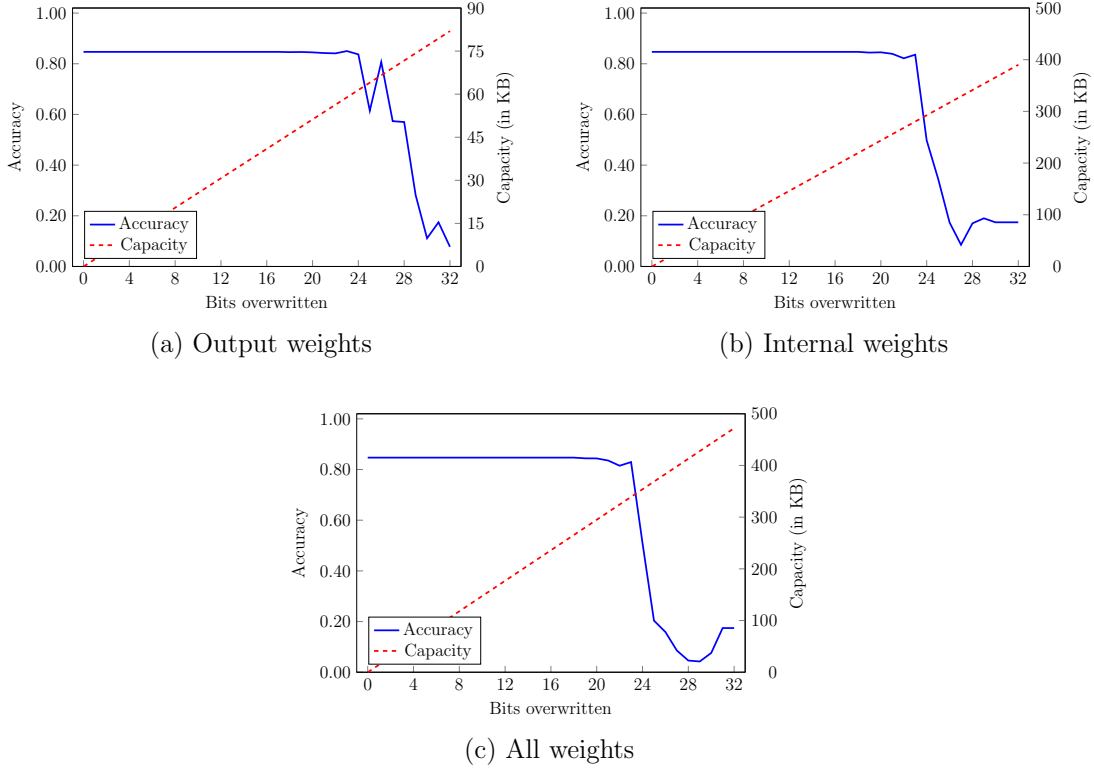


Figure 11: ACGAN steganographic capacity graphs

Figure 23 in the appendix gives results the steganographic capacity results for each of the 4 individual layers in ACGAN. These graphs follow a similar pattern as the graphs in Figure 11, and hence we observe no significant differences between the individual layers.

The ACGAN discriminator has 20,490 weights in the output layer and 97,536 weights in the hidden layers, for a total of 118,026 weights. Based on a per-weight capacity of 20 bits, the total steganographic capacity is 295.065 KB.

4.11 Discussion

We summarize our steganographic capacity findings in Table 12 and, in bar graph form, in Figure 12. Of the models tested, SVM has the highest capacity per weight, which implies that this particular model requires the least precision in its weights. This is not surprising, given that the SMO algorithm that is used to train SVMs relies on the fact that low precision suffices. Of the pre-trained

transfer learning models, InceptionV3 has the highest capacity per-weight, with respect to trained weights.

Table 12: Summary of results

Model	Layers	Weights	Steganographic capacity	
			Bits per weight	Total
LR	All	2560	22	7.04 KB
SVM	All	26,703	27	90.12 KB
MLP	All	34,148	19	81.10 KB
CNN	All	1,489,674	20	3.72 MB
LSTM	All	1,119,626	24	3.36 MB
VGG16	Trained	5130	21	13.847 KB
DenseNet121	Trained	700,106	20	1.75 MB
InceptionV3	Trained	2,107,392	25	6.59 MB
Xception	Trained	34,176	20	85.44 KB
ACGAN	Discriminator	118,026	20	295.07 KB

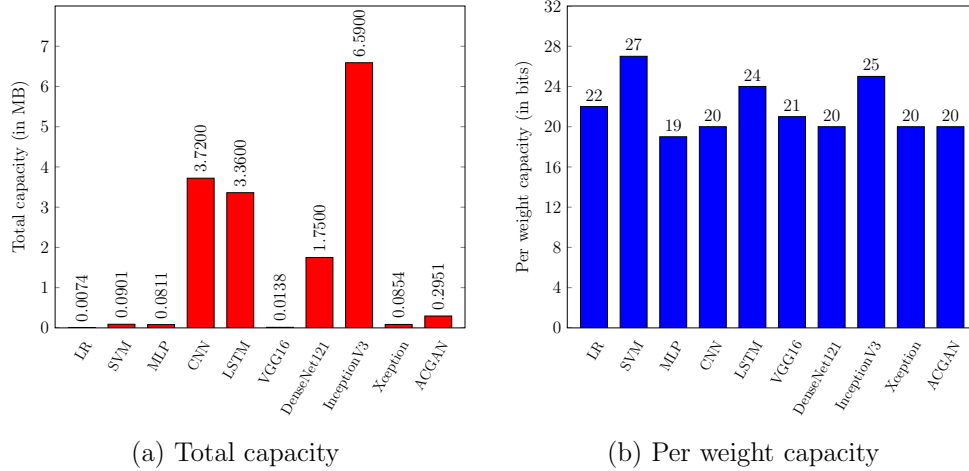


Figure 12: Bar graphs of capacity results

Note that the numbers in Table 12 and Figure 12 for the pre-trained models (VGG16, DenseNet121, InceptionV3, Xception) only include the trained weights, that is, the weights that were retrained for the specific malware classification problem under consideration. In Section 4.8, we found that the per-weight capacity for the pre-trained layers of the InceptionV3 model was just 14 bits, as compared to 25 bits for its trained weights. In spite of this low per-weight capacity, the number of pre-trained weights in InceptionV3 is large, and hence the steganographic capacity is large—if we consider all weights, the capacity is 44.74 MB. Similarly, in Section 4.6 we showed that if we consider all weights of the VGG16 model, it has also has an extremely high steganographic capacity at 36.80 MB.

5 Conclusion

The primary goal of this research was to determine reasonable lower bounds for the steganographic capacity of a representative sample of learning models. Each model was trained on a dataset of more than 15,000 malware executables from 10 families, with more than 1000 samples per family.

All of the trained learning models underwent a similar testing procedure: We first determined the accuracy of a model on the test set, then we embedded information in the n low-order bits of the weights, for $n = 1, 2, \dots, 32$, and we recomputed the classification accuracy for each n . For generic deep learning models, we experimented with the output layer weights, the hidden layer weights, and all of the weights, while for pre-trained models, we considered the trained weights. The results were fairly consistent across all models, in that a substantial number of bits per weight can be used to hide information, with minimal effect on the accuracy. In addition, at some point, the accuracy of all models dropped precipitously, indicating a minimum level of required precision. These results were also reasonably consistent across the various layers of the models, with the only notable exception being the pre-trained weights of the InceptionV3 model, which had a lower per-weight steganographic capacity.

Our experimental results show that the steganographic capacity of the models we tested is surprisingly high. This is potentially a significant security issue, since such models are ubiquitous, and hence it is to be expected that attackers will try to take advantage of them. Embedding, say, malware in a learning model offers an attack vector that is practical, and could be highly effective in practice.

It would be wise to reduce the steganographic capacity of learning models. Our results indicate that standard 32-bit weights do not yield a significant improvement in accuracy over what could be achieved with, say, 16-bit weights, and for some models, 8-bit weights would be more than sufficient.

Further research into other popular deep learning models would be worthwhile. Also, training models on different types of problems—including classification problems of varying levels of difficulty—would tell us whether the capacity of a specific model varies with the difficulty of the problem. Additional analysis of the pre-trained weights of transfer learning models would be interesting. Research on compressed models that use smaller numbers of bits to store each weight would be of practical significance.

Dropout regularization in, say, MLPs (equivalently, cutouts in CNNs) is used to force more neurons to be active in training, which can be very effective in reducing overfitting. It would be interesting to determine whether such regularization techniques also affect the precision of trained weights, which can be measured via the steganographic capacity experiments presented in this paper.

Another area for further investigation would be to combine some aspects of the steganographic capacity approach considered in this paper with the work in [33], where information is hidden in weights that are (essentially) unused by the model. By combining both of these techniques, we could obtain even larger

steganographic capacities for learning models. Finally, it would be interesting—although challenging—to obtain tight upper bounds on the minimum size of various models, with the goal of eliminating any usable steganographic capacity.

References

- [1] Monika Agarwal. Text steganographic approaches: A comparison. *International Journal of Network Security & Its Applications*, 5(1):91–106, 2013.
- [2] James Anthony. 60 notable machine learning statistics: 2021/2022 market share & data analysis. <https://financesonline.com/machine-learning-statistics/>, 2022.
- [3] Avijeet Biswal. Convolutional neural network tutorial. <https://www.simplilearn.com/tutorials/deep-learning-tutorial/convolutional-neural-network-tutorial/>, 2022.
- [4] Lewis Carroll. *Alice’s Adventures in Wonderland*. Macmillan, 1865. <https://www.gutenberg.org/ebooks/11>.
- [5] Francois Chollet. Xception: Deep learning with depthwise separable convolutions. <https://arxiv.org/abs/1610.02357>, 2017.
- [6] Nikita Duggal. Top 10 machine learning applications and examples in 2022. <https://www.simplilearn.com/tutorials/machine-learning-tutorial/machine-learning-applications-in-2022/>, 2022.
- [7] Andrada Fiscutean. Steganography explained and how to protect against it. <https://www.csoonline.com/article/3632146/steganography-explained-and-how-to-protect-against-it/>, 2021.
- [8] Ian J. Goodfellow, Jean Pouget-Abadie, Mehdi Mirza, Bing Xu, David Warde-Farley, Sherjil Ozair, Aaron Courville, and Yoshua Bengio. Generative adversarial nets. In *Proceedings of the 27th International Conference on Neural Information Processing Systems*, volume 2 of *NIPS’14*, pages 2672–2680, 2014.
- [9] Arpit Gupta. Alexa blogs: How Alexa is learning to converse more naturally. <https://developer.amazon.com/blogs/alexa/post/15bf7d2a-5e5c-4d43-90ae-c2596c9cc3a6>, 2018.
- [10] Gao Huang, Zhuang Liu, Laurens van der Maaten, and Kilian Q. Weinberger. Densely connected convolutional networks. <https://arxiv.org/abs/1608.06993>, 2018.
- [11] Pranav Khaitan. Google AI blog: Chat smarter with Allo. <https://ai.googleblog.com/2016/05/chat-smarter-with-allo.html>, 2016.
- [12] Samuel Kim. Pe header analysis for malware detection. Master’s thesis, San Jose State University, 2018.

- [13] Sudhir Kumar. Kaggle: Linear regression tutorial. <https://www.kaggle.com/code/sudhirnl7/linear-regression-tutorial>, 2020.
- [14] Steven Levy. The iBrain is here—and it’s already inside your phone. *Wired*. <https://www.wired.com/2016/08/an-exclusive-look-at-how-ai-and-machine-learning-works/>, 2016.
- [15] Tao Liu, Zihao Liu, Qi Liu, Wujie Wen, Wenyao Xu, and Ming Li. StegoNet: Turn deep neural network into a stegomalware. In *Proceedings 36th Annual Computer Security Applications Conference, ACSAC*, pages 928–938, 2020. <https://cse.buffalo.edu/~wenyaoxu/papers/conference/xu-acnac2020.pdf>.
- [16] Microsoft. Trojan:Win32/VB. <https://www.microsoft.com/en-us/wdsi/threats/malware-encyclopedia/item/trojan-win32/vb>, 2007.
- [17] Microsoft. VirTool:Win32/CeeInject. <https://www.microsoft.com/en-us/wdsi/threats/malware-encyclopedia/item/virtool-win32/ceeinject>, 2007.
- [18] Microsoft. Win32/Renos. <https://www.microsoft.com/en-us/wdsi/threats/malware-encyclopedia/item/win32/renos>, 2007.
- [19] Microsoft. Trojan:Win32/BHO.BO. <https://www.microsoft.com/en-us/wdsi/threats/malware-encyclopedia/item/trojan-win32/bho-bo>, 2009.
- [20] Microsoft. VirTool:Win32/VBInject. <https://www.microsoft.com/en-us/wdsi/threats/malware-encyclopedia/item/virtool-win32/vbinject>, 2010.
- [21] Microsoft. Win32/Vobfus. <https://www.microsoft.com/en-us/wdsi/threats/malware-encyclopedia/item/win32/vobfus>, 2010.
- [22] Microsoft. Win32/Winwebsec. <https://www.microsoft.com/en-us/wdsi/threats/malware-encyclopedia/item/win32/winwebsec>, 2010.
- [23] Microsoft. Trojan:Win32/Startpage. <https://www.microsoft.com/en-us/wdsi/threats/malware-encyclopedia/item/trojan-win32/startpage>, 2011.
- [24] Microsoft. Win32/OnLineGames. <https://www.microsoft.com/en-us/wdsi/threats/malware-encyclopedia/item/win32/onlinegames>, 2015.
- [25] Microsoft. Adware:Win32/Adload. <https://www.microsoft.com/en-us/wdsi/threats/malware-encyclopedia/item/adware-win32/adload>, 2018.
- [26] Jay Selig. What is machine learning? a definition. <https://www.expert.ai/blog/machine-learning-definition/>, 2022.
- [27] Karen Simonyan and Andrew Zisserman. Very deep convolutional networks for large-scale image recognition. <https://arxiv.org/abs/1409.1556>, 2015.
- [28] Mark Stamp. *Information Security: Principles and Practice*. Wiley, 3rd edition, 2021.
- [29] Mark Stamp. *Introduction to Machine Learning with Applications in Information Security*. Chapman and Hall/CRC, 2nd edition, 2022.

- [30] James Stanger. The ancient practice of steganography: What is it, how is it used and why do cybersecurity pros need to understand it. <https://www.comptia.org/blog/what-is-steganography>, 2020.
- [31] Christian Szegedy, Wei Liu, Yangqing Jia, Pierre Sermanet, Scott Reed, Dragomir Anguelov, Dumitru Erhan, Vincent Vanhoucke, and Andrew Rabinovich. Going deeper with convolutions. <https://arxiv.org/abs/1409.4842>, 2014.
- [32] Hind Taud and Jean-Francois Mas. Multilayer perceptron (MLP). In Mar´ia Teresa Camacho Olmedo, Martin Paegelow, Jean-Francois Mas, and Francisco Escobar, editors, *Geomatic Approaches for Modeling Land Change Scenarios*, pages 451–455. Springer, 2018.
- [33] Zhi Wang, Chaoge Liu, and Xiang Cui. EvilModel: Hiding malware inside of neural network models. In *2021 IEEE Symposium on Computers and Communications, ISCC*, pages 1–7, 2021. <https://arxiv.org/abs/2107.08590>.
- [34] Zhi Wang, Chaoge Liu, Xiang Cui, Jie Yin, and Xutong Wang. EvilModel 2.0: Bringing neural network models into malware attacks. *Computers & Security*, 120:102807, 2022.
- [35] Yonghui Wu et al. Google’s neural machine translation system: Bridging the gap between human and machine translation. <https://arxiv.org/abs/1609.08144>, 2016.
- [36] Lei Zhang, Dong Li, Olha Jurečková, and Mark Stamp. Steganographic capacity of deep learning models. <https://arxiv.org/abs/2306.17189>, 2023.

Appendix

In this appendix, we provide confusion matrices for each of the models analyzed in this paper. We observe that, in general, VB and VBInject are consistently the most difficult families to distinguish. We also provide additional steganographic capacity graphs for selected models.

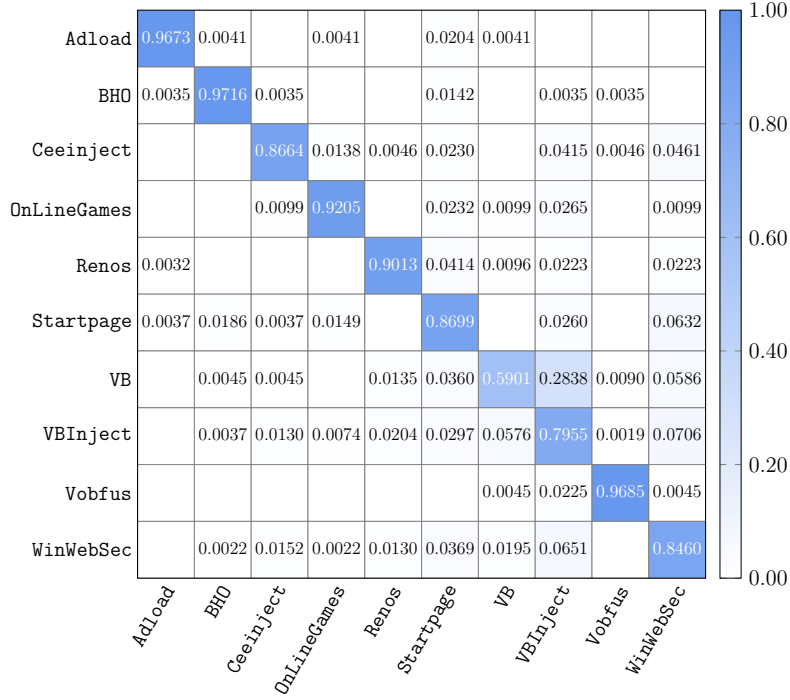


Figure 13: LR confusion matrix

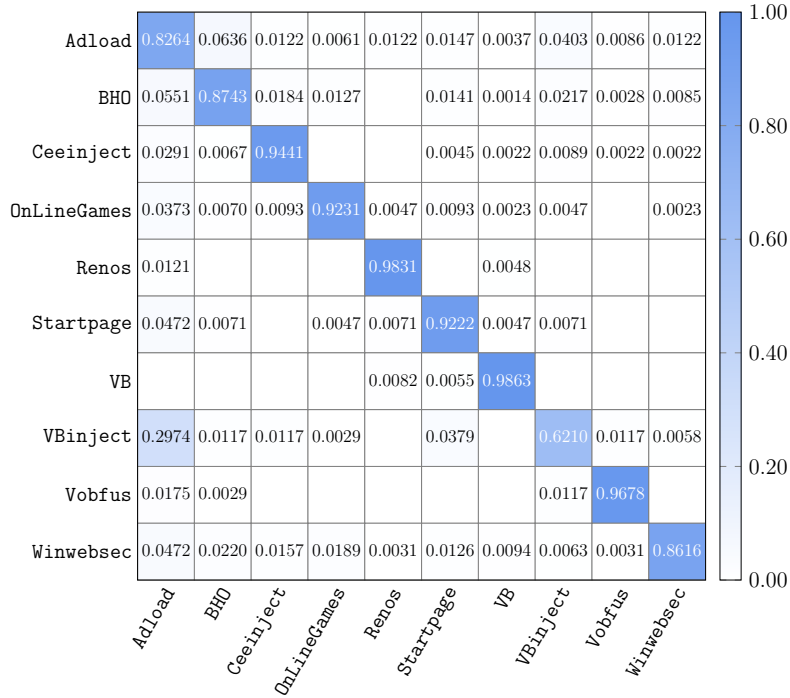


Figure 14: SVM confusion matrix

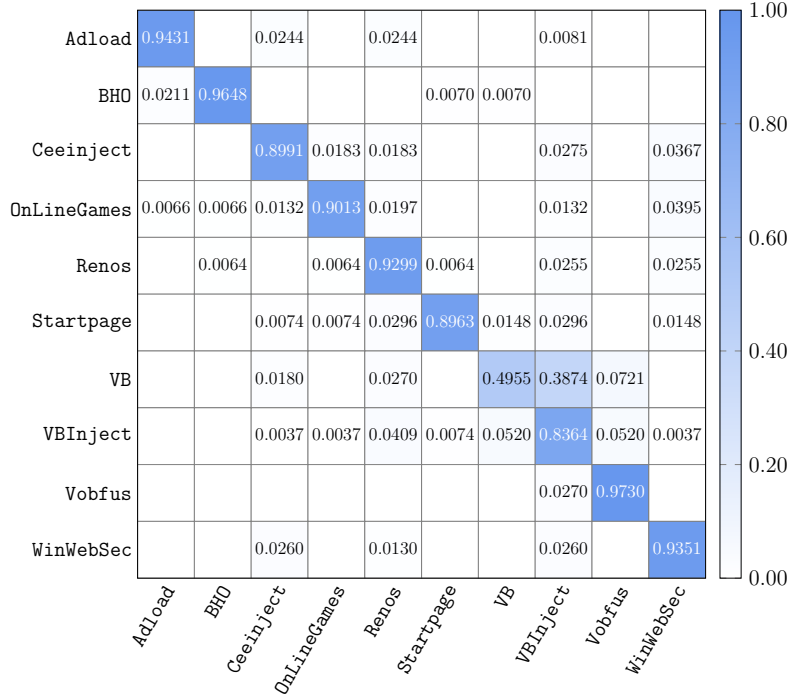


Figure 15: CNN confusion matrix

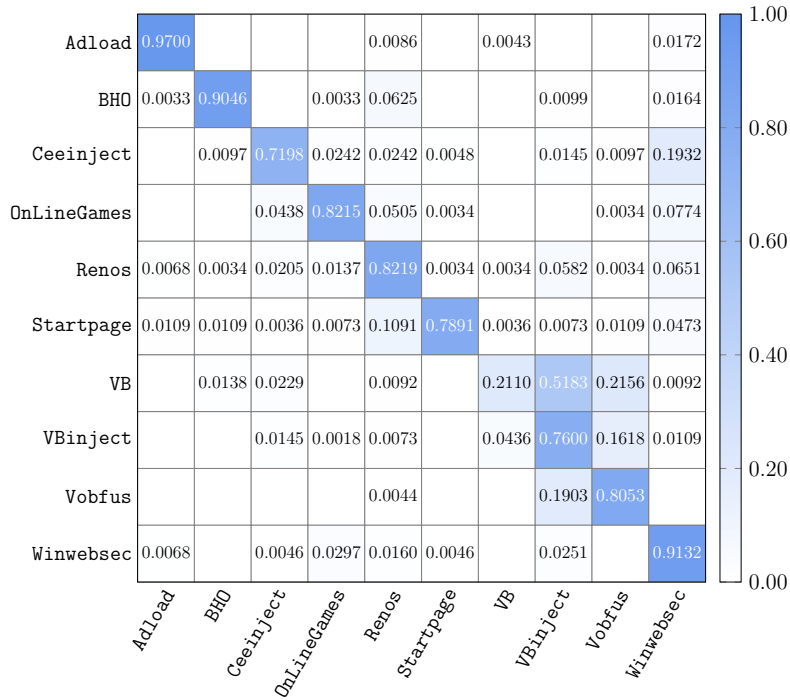


Figure 16: LSTM confusion matrix

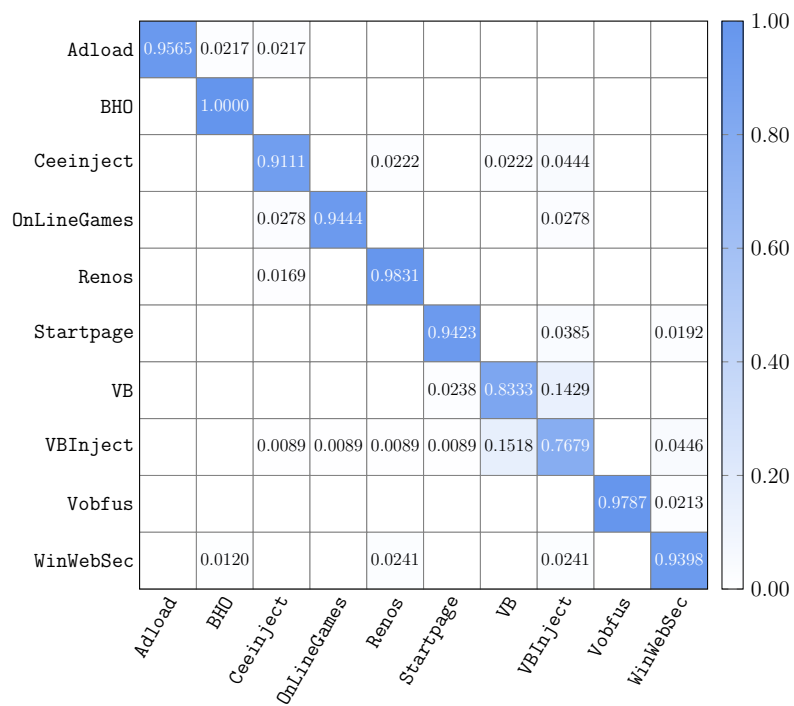


Figure 17: VGG16 confusion matrix

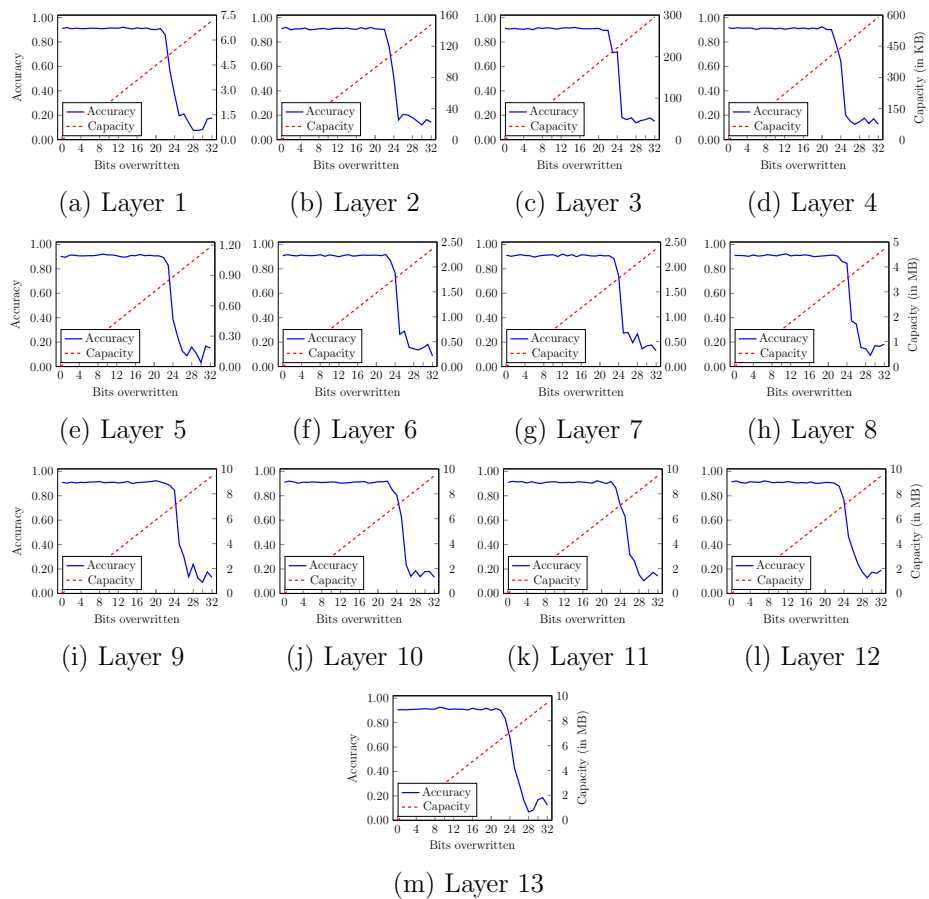


Figure 18: VGG16 capacity graphs for individual layers

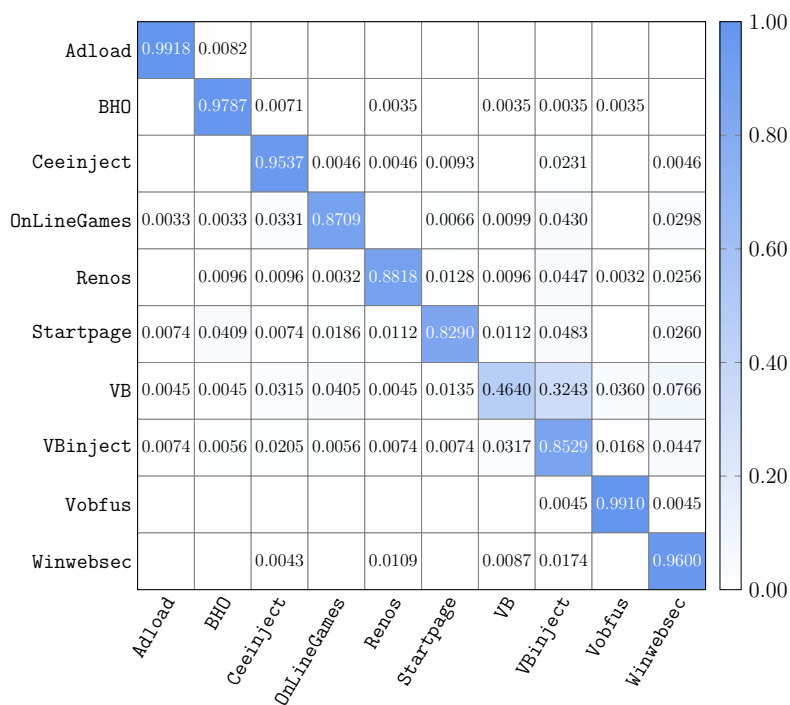


Figure 19: DenseNet121 confusion matrix

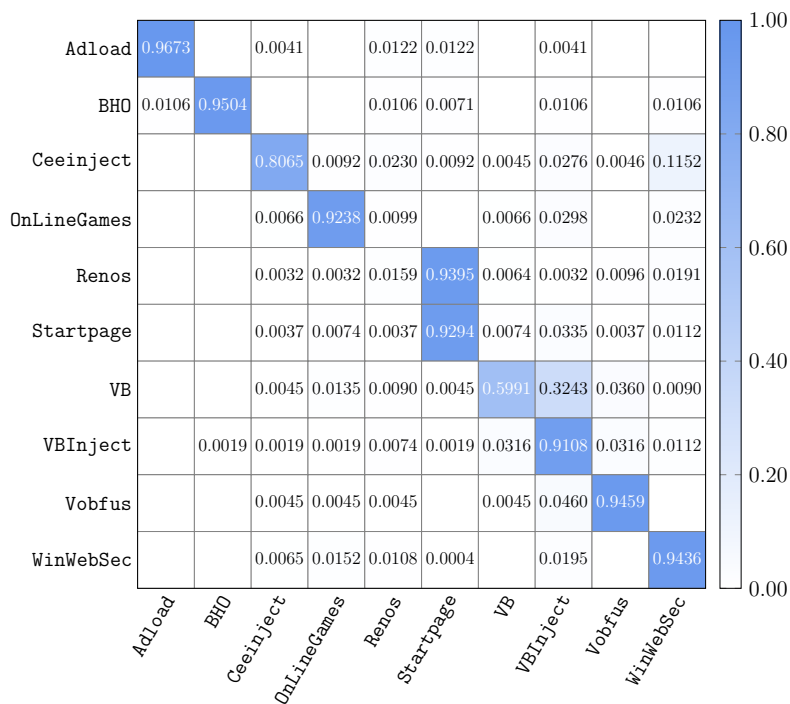


Figure 20: InceptionV3 confusion matrix

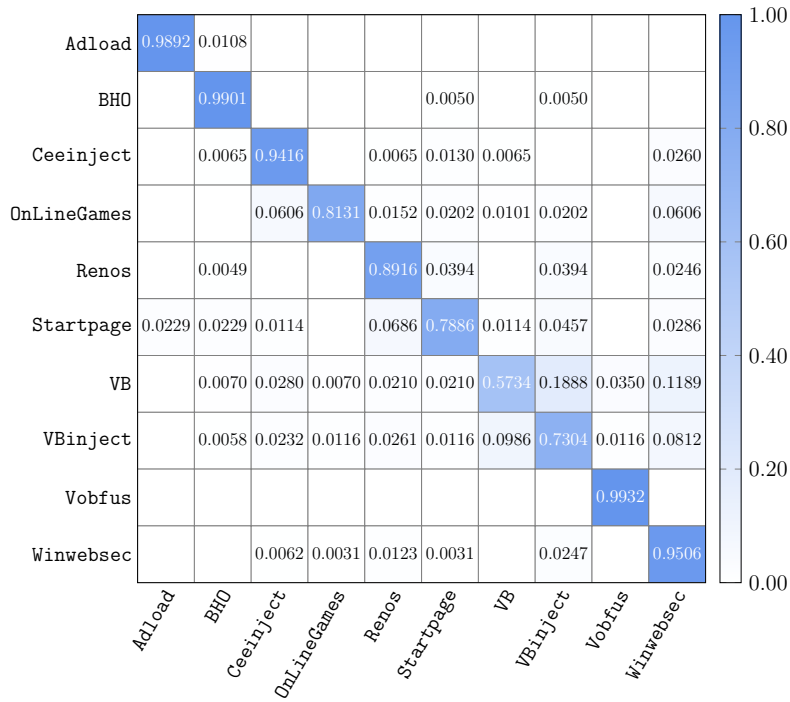


Figure 21: Xception confusion matrix

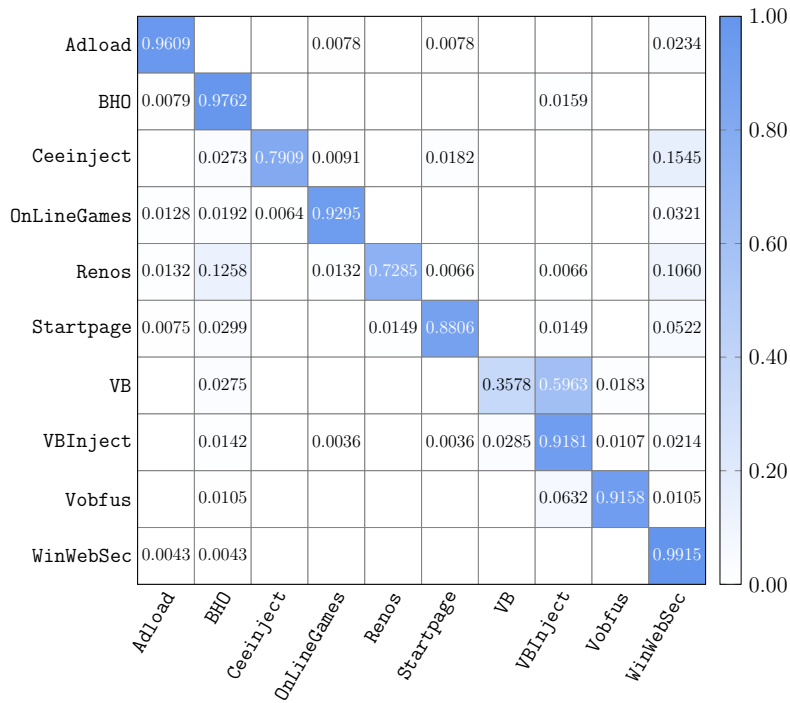
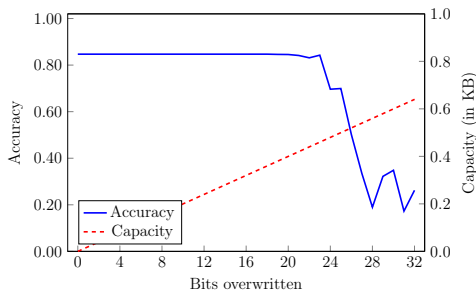
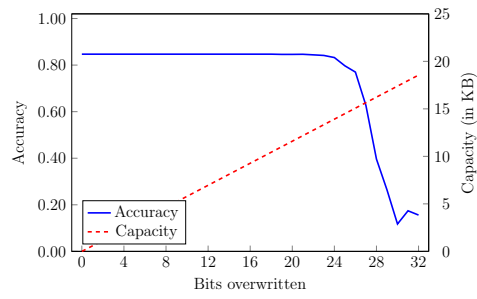


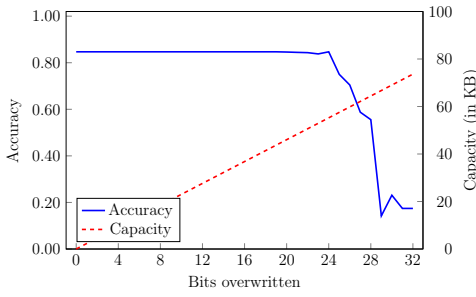
Figure 22: ACGAN confusion matrix



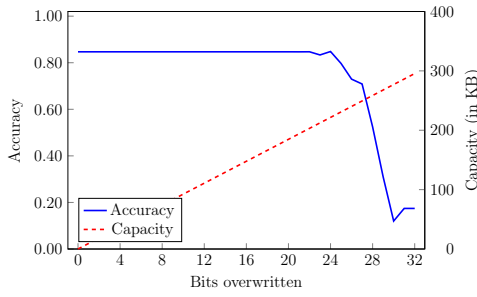
(a) Layer 1



(b) Layer 2



(c) Layer 3



(d) Layer 4

Figure 23: ACGAN capacity graphs for individual layers